Contrib Mineral Petrol (1994) 118:79–91

J. F. G. Wilkinson · H. D. Hensel

Nephelines and analcimes in some alkaline igneous rocks

Received: 20 September 1993 / Accepted: 9 May 1994

Abstract The paper presents electron microprobe analyses of nephelines and analcimes in alkaline igneous rocks ranging from theralite and basanite to mugearite and tinguaite. With few exceptions, the nephelines are Si-rich types whose Qz (quartz) components exceed those defining the limits of excess SiO_2 in solid solution in the Ne-Ks-Qz-H_2O system at 700° C and 1 kbar P_{H_2O}. Unlike the nephelines in the basanites which show only limited grain-to-grain compositional variation, those in theralites and tinguaites from the differentiated Square Top intrusion, New South Wales, and in a New Zealand tinguaite vary significantly in Ne (nepheline), Ks (kalsilite) and Qz, even within individual samples, and they also may be strongly zoned. The rims of zoned nephelines are enriched in Si and Fe^{3+}, relative to core compositions. These zoning trends contrast with the composional trend of successive "bulk" nepheline fractions in the Square Top sequence theralite → tinguaite whereby Qz decreases. The nephelines coexist with high-temperature alkali feldspars. In the Ne-Ks-Qz system they plot on the Ne side of the Barth compositional join defined by the omission solid solution series with end-members $K_2Na_6Al_8Si_8O_{32}$ (the Buerger ideal composition; $Ne_{75}Ks_{25}$ mol%) and $\square_2Na_6Al_6Si_{10}O_{32}$ ($\square$ = cavity cation vacancy). The compositions of most natural nephelines are restricted to the field defined by Ne and the Barth join, compositions more K-rich than the ideal composition being relatively rare. The compositions of nephelines on the Ne side of the join are controlled by a number of factors which include the physical conditions attending nepheline crystallization and the compositions of the alkaline hosts. Interstitial analcimes from the Square Top intrusion display extensive $NaAl \rightleftharpoons Si$ substitution and their compositions extend from analcime of natrolite composition to compositions slightly more Si-rich than "ideal" $NaAlSi_2O_6$. Groundmass analcimes in the basanites, mugearite and New Zealand tinguaite have relatively constant compositions which approach stoichiometric $NaAlSi_2O_6$. An unusually Si-rich deuteric analcime (60.2% SiO_2) is also present in vugs in the New Zealand tinguaite. Experimental and other evidence, including P/T data defining the coexistence of analcime and silica-undersaturated silicate melt in the $NaAlSiO_4$–$KAlSiO_4$–SiO_2–H_2O system, and inferred solidus temperatures of the various hosts (they would have exceeded the stability range of analcime) preclude a primary magmatic origin for the interstitial and groundmass analcimes. These are interpreted as subsolidus phases produced by nepheline interaction with deuteric and/or hydrothermal fluids. Analyses of nephelines and their derivative analcimes indicate that the latter may form from both Si-rich and more Si-poor nephelines.

J. F. G. Wilkinson (✉)
Department of Geology and Geophysics,
University of New England, Armidale 2351, Australia

H. D. Hensel
Department of Geology, Australian National University,
Canberra 2601, Australia

Editorial responsibility: R. A. Binns

Introduction

Nepheline and analcime are potential accessory or essential phases in a wide range of nepheline-normative igneous rocks. Nepheline is the most widespread and abundant of the feldspathoids and consequently more is known of the variations in its composition with paragenesis than other feldspathoids. There are, however, very few data on nepheline fractionation trends resulting from the differentiation of alkaline magmas.

Although analcime is in all respects a valid member of the zeolite mineral group, in chemistry and paragenesis it has close affinities with the feldspathoids, especially nepheline with which it commonly coexists. However, unlike nephelines in igneous parageneses, the

origin of some "igneous" analcimes is controversial and, except for the data of Henderson and Gibb (1983), relations between coexisting nephelines and analcimes are only poorly known.

Some analcimes in igneous rocks are clearly alteration products of feldspars and feldspathoids or produced by hydrothermal processes. Much more puzzling is the origin of euhedral analcime phenocrysts in some alkaline lavas. Mainly on petrographic grounds these have been traditionally interpreted as a primary magmatic phase. Experimental studies in the system $NaAlSiO_4$-$KAlSiO_4$-SiO_2-H_2O and its sodic subsystems have demonstrated that analcime can coexist with silica-undersaturated salic melts at temperatures between 600 and 640° C in the pressure range 5–13 kbar (Peters et al. 1966; Kim and Burley 1971; Roux and Hamilton 1976). Consequently, analcime phenocrysts in analcime-phyric trachytes and phonolites (blairmorites and shackanites) and some hydrous lamprophyres have been interpreted as intratelluric high-pressure phases (e.g. Woolley and Symes 1976; Ferguson and Edgar 1978; Edgar 1979; Luhr and Kyser 1989; Pearce 1993). Proponents of an alternative origin for these phenocrysts and also those in more mafic potassic volcanics ($K_2O/Na_2O \geq 1$) have argued that the analcimes are secondary and represent ion- exchanged leucites (e.g. Nakamura and Yoder 1974; Wilkinson 1977; Comin-Chiaramonti et al. 1979; Karlsson and Clayton 1991). Leucite is the preferred precursor to analcime because of their similar crystal morphologies and the ease with which leucite transforms to analcime at very low pressures and at subsolidus temperatures by the ion-exchange reaction $KAlSi_2O_6 + Na^+ + H_2O = NaAlSi_2O_6 \cdot H_2O + K^+$ (Gupta and Fyfe 1975).

Historically, interstitial analcime in relatively K poor hosts such as teschenites and crinanites has often been considered primary because evidence of a suitable precursor phase is generally lacking. Relict

Table 1 Analyses of nepheline- and/or analcime-bearing hosts. [**M* 100 Mg/(Mg + Fe^{2+}), *AN* 100 *an*/(*ab* + *an*), *DI* differentiation index $\sum$ *or*, *ab*, *ne*. *1* Analcime theralite ST28, close to lower contact of Square Top intrusion, 2 miles west of Nundle, New South Wales (Wilkinson 1965), *2* analcime tinguaite ST12 from top of Square Top intrusion (locality as for 1 above), *3* analcime tinguaite, Portobello, Otago Harbour, New Zealand (Wilkinson 1968), *4, 5* analcime-nepheline basanites (R9687 and R18720, respectively), Mount Nombi Station, west of Gunnedah, New South Wales. Analyst J. Bedford, University of New England, *6* analcime mugearite R21692, from flow 1 km east of Spring Mount, north-eastern New South Wales (Wilkinson and Hensel 1991). *or* orthoclase, *ab* albite, *an* anorthite, *ne* nepheline, *ac* acmite, *di* diopside, *wo* wollastonite, *ol* olivine, *mt* magnetite, *hm* hematite, *il* ilmenite, *ap* apatite, *cc* calcite]

	Square Top		Portobello	Nombi		Spring Mount
Analysis number	1	2	3	4	5	6
SiO_2	44.90	52.61	54.76	40.94	41.80	46.32
TiO_2	2.13	0.38	0.02	2.53	2.51	1.61
Al_2O_3	14.97	18.88	19.63	11.73	12.19	15.85
Fe_2O_3	2.62	4.06	4.34	4.79	4.69	4.94
FeO	8.26	1.72	1.28	8.29	8.35	6.38
MnO	0.15	0.11	0.21	0.20	0.20	0.21
MgO	8.45	1.62	0.07	11.19	10.65	4.17
CaO	9.08	2.43	1.10	10.87	10.79	5.52
Na_2O	5.02	8.93	9.18	2.63	3.19	4.68
K_2O	1.72	4.08	4.65	0.80	0.67	5.48
H_2O	1.59	4.39	4.17	4.27	3.36	3.37
P_2O_5	0.97	0.55	0.06	0.77	0.75	1.15
CO_2	–	–	0.65	–	–	0.15
Total	99.86	99.76	100.12	[a]99.30	[b]99.57	99.83
			CIPW norms			
or	10.0	23.9	27.5	5.0	3.9	20.0
ab	13.4	34.1	39.9	9.4	12.1	27.3
an	13.3	–	–	17.8	17.2	12.0
ne	15.8	21.9	19.1	6.8	8.0	6.8
ac	–	0.9	2.3	–	–	–
di	20.4	6.5	0.2	25.5	25.8	5.6
wo	–	–	0.2	–	–	–
ol	15.2	0.7	–	16.8	15.9	9.4
mt	3.7	4.9	4.8	7.0	6.7	7.2
hm	–	0.3	0.3	–	–	–
il	4.1	0.8	tr.	4.9	4.7	3.0
ap	2.3	1.3	0.1	1.7	1.7	2.7
cc	–	–	1.5	–	–	0.3
etc.	1.6	4.4	4.2	4.3	3.4	5.5
Total	99.8	99.7	100.1	99.2	99.4	99.8
**M*	64.6	62.7	8.7	70.6	69.5	53.8
**AN*	49.8	–	–	65.4	58.7	30.5
**DI*	39.2	79.9	86.5	21.2	24.0	54.1
K_2O/Na_2O	0.34	0.46	0.51	0.30	0.21	0.72

[a] Total includes 0.06 Cr_2O_3, 0.03 NiO, 0.08 BaO, 0.12 SrO (R9687)
[b] Total includes 0.06 Cr_2O_3, 0.04 NiO, 0.22 BaO, 0.10 SrO (R18720)

Si-rich nephelines in interstitial analcimes have now been documented by Henderson and Gibb (1983) who proposed that the analcime derived from late-crystallizing Si-rich nepheline by subsolidus reactions involving deuteric or hydrothermal fluids.

Finally, analcime may constitute the colourless isotropic base of some monchiquites, tinguaites and analcimites. This microscopically structureless "groundmass" analcime has been regarded as either primary (Pirsson 1896; Washington 1898; Coleman 1899) or a devitrification product of glass (Rock 1977).

In this study we examine several aspects of the nephelines and analcimes in a variety of alkaline hosts ranging in composition from theralite and basanite to mugearite and tinguaite, including: (1) nepheline fractionation trends in a differentiation series theralite → tinguaite and the relevance of these to natural nepheline compositions; (2) the primary or secondary nature of interstitial and groundmass analcimes; (3) relations between nephelines and possible derivative analcimes.

Petrography and mineralogy

In this summary end-member mineral compositions are given as mol% (pyroxene nomenclature follows Morimoto, 1988) and oxide abundances in wt%. Bracketed compositions of Square Top minerals are those of mineral separates (Wilkinson 1965, 1966). Throughout the text nepheline, analcime and feldspar compositions are given as mol%, unless stated otherwise. The CIPW normative minerals (wt%) are in italics, non-capitalised, see Table 1 for abbreviations.

Electron microprobe analyses were carried out on a Camebax Microbeam (Cameca) instrument at the Research School of Earth Sciences, Australian National University, Canberra, following procedures detailed by Ware (1991). Electron microprobe analysis circumvents the analytical problems in the earlier studies, posed by very difficult mineral separations (Wilkinson 1965, 1968). Particular care was taken to minimize alkali loss from nepheline and analcime. Nepheline and analcime analyses were generally considered acceptable if $Si + Al + Fe^{3+}$ summed to 4.00 ± 0.01 (8O for nepheline) and 3.00 ± 0.01 (6O for analcime) and if $2Ca + Na + K \simeq Al + Fe^{3+}$ (Bannister and Hey 1931).

Square Top intrusion, Nundle, New South Wales

The strongly differentiated Palaeocene Square Top intrusion is a small plug-like body which reveals in its petrography and chemistry a continuous passage from analcime theralite (Table 1, No. 1) to analcime tinguaite (Table 1, No. 2). Analyses of three additional samples investigated in this study (theralite ST20 and tinguaites ST40 and ST16) are listed by Wilkinson (1965, Table 1).

Theralites

Theralites ST28 (DI = 39.2; *DI* = $\sum$ *or, ab, ne*) and ST20 (DI = 52.4) are medium-grained rocks with phenocrysts of Mg-rich diopside (maximum grain dimensions 4 mm; ST28 composition

Table 2 Analyses of nephelines. *1* Most Si-rich nepheline in analcime theralite ST28 (Table 1, No. 1), *2* most Si-rich nepheline in analcime theralite ST20, *3* most Si-poor nepheline in analcime tinguaite ST40, *4C, 5R* core and rim, respectively, of zoned nepheline phenocryst in analcime tinguaite ST12 (Table 1, No. 2), *6, 7* Si-poor and Si-rich nephelines in the Portobello analcime tinguaite (Table 1, No. 3), *8, 9* average nepheline compositions (each based on analyses of 5 nephelines) in Nombi analcime-nepheline basanites (Table 1, Nos. 4 and 5, respectively)]

	Square Top					Portobello		Nombi	
Analysis number	Theralites 1	2	Tinguaites 3	4C → 5R		6	7	8	9
SiO_2	51.82	51.95	45.97	44.71	47.66	45.83	49.27	45.59[b] (0.75)	48.23 (0.27)
Al_2O_3	29.81	28.53	31.96	32.95	30.79	32.64	29.56	32.46 (0.38)	31.40 (0.44)
Fe_2O_3	0.40	0.81	0.42	0.89	1.23	0.49	0.93	0.61 (0.08)	0.51 (0.12)
CaO	[a]tr.	tr.	tr.	tr.	tr.	0.27	tr.	1.22 (0.54)	0.77 (0.04)
Na_2O	16.65	16.45	16.92	17.23	16.98	17.05	16.26	16.25 (0.24)	16.02 (0.00)
K_2O	2.15	1.83	4.07	4.56	3.40	3.73	3.07	3.31 (0.10)	3.13 (0.20)
Total	100.83	99.57	99.34	100.34	100.06	100.01	99.09	99.44	100.06
Cell formulae for 8 (O)									
Si	2.378	2.411	2.190	2.125	2.246	2.168	2.325	2.166	2.258
Al	1.612 4.00	1.560 4.00	1.795 4.00	1.846 4.00	1.710 4.00	1.818 4.00	1.644 4.00	1.817 4.01	1.732 4.01
Fe^{3+}	0.014	0.028	0.015	0.032	0.044	0.018	0.033	0.022	0.018
Ca	–	–	–	–	–	0.014	–	0.062	0.039
Na	1.481	1.480	1.563	1.588	1.552	1.564	1.487	1.497	1.454
K	0.126	0.110	0.247	0.276	0.204	0.225	0.185	0.200	0.187
$Al + Fe^{3+}$	1.63	1.59	1.81	1.88	1.75	1.84	1.68	1.84	1.75
$2Ca + Na + K$	1.61	1.59	1.81	1.86	1.76	1.82	1.67	1.82	1.72
Mol%									
Ne	62.3	61.4	71.4	74.8	69.1	73.0	64.1	73.3	66.7
Ks	5.3	4.5	11.3	13.0	9.1	10.5	7.9	9.8	8.5
Qz	32.4	34.1	17.3	12.2	21.8	16.5	28.0	16.9	24.8

[a] For Tables 2, 3 tr. = trace ($Fe_2O_3 < 0.09$, $CaO < 0.05$, $K_2O < 0.05$)
[b] ($\pm 1\sigma$)

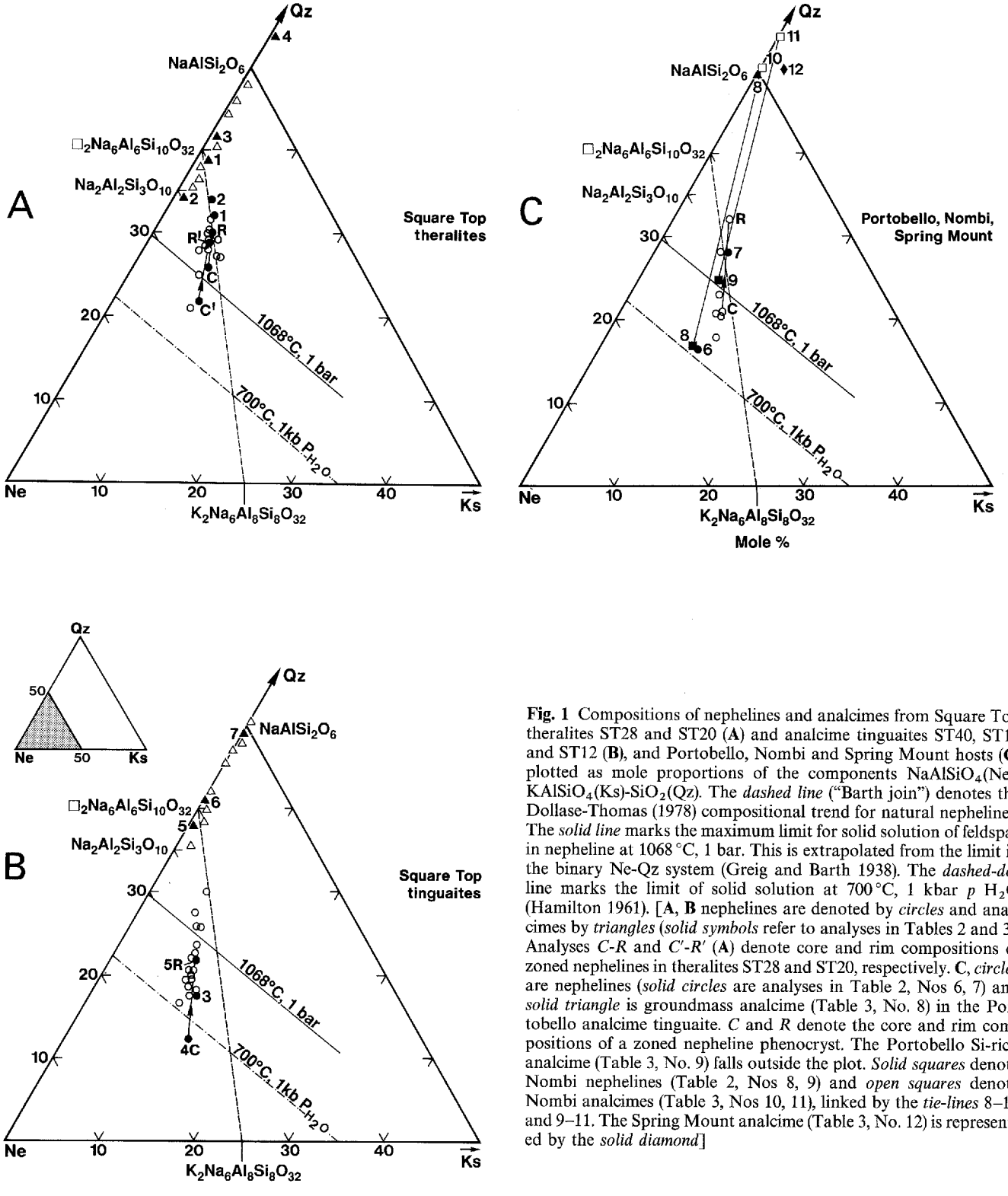

Fig. 1 Compositions of nephelines and analcimes from Square Top theralites ST28 and ST20 (**A**) and analcime tinguaites ST40, ST16 and ST12 (**B**), and Portobello, Nombi and Spring Mount hosts (**C**) plotted as mole proportions of the components $NaAlSiO_4$(Ne)-$KAlSiO_4$(Ks)-SiO_2(Qz). The *dashed line* ("Barth join") denotes the Dollase-Thomas (1978) compositional trend for natural nephelines. The *solid line* marks the maximum limit for solid solution of feldspar in nepheline at 1068 °C, 1 bar. This is extrapolated from the limit in the binary Ne-Qz system (Greig and Barth 1938). The *dashed-dot* line marks the limit of solid solution at 700 °C, 1 kbar $p\ H_2O$ (Hamilton 1961). [**A**, **B** nephelines are denoted by *circles* and analcimes by *triangles* (*solid symbols* refer to analyses in Tables 2 and 3). Analyses *C-R* and *C'-R'* (**A**) denote core and rim compositions of zoned nephelines in theralites ST28 and ST20, respectively. **C**, *circles* are nephelines (*solid circles* are analyses in Table 2, Nos 6, 7) and *solid triangle* is groundmass analcime (Table 3, No. 8) in the Portobello analcime tinguaite. *C* and *R* denote the core and rim compositions of a zoned nepheline phenocryst. The Portobello Si-rich analcime (Table 3, No. 9) falls outside the plot. *Solid squares* denote Nombi nephelines (Table 2, Nos 8, 9) and *open squares* denote Nombi analcimes (Table 3, Nos 10, 11), linked by the *tie-lines* 8–10 and 9–11. The Spring Mount analcime (Table 3, No. 12) is represented by the *solid diamond*]

$Ca_{47}Mg_{40}\sum Fe_{13}$ where $\sum Fe = Fe^{2+} + Fe^{3+} + Mn$), zoned olivine (2 mm; Fo_{71} in ST28, Fo_{70} in ST20), plagioclase (2 mm; $Ab_{44}An_{51}Or_5$ in ST28, $Ab_{50}An_{41}Or_9$ in ST20) and nepheline (2 mm). In zoned plagioclases, core compositions range from labradorite $Ab_{33}An_{65}Or_2$ to potash oligoclase $Ab_{68}An_{22}Or_{10}$, with outer zones either anorthoclase $Or_{32}Ab_{60}An_8$ or sanidine $Or_{57}Ab_{42}An_1$. Alkali feldspars range in composition from $Ab_{58}Or_{40}An_2$ to $Ab_{38}Or_{62}$.

Most of the nepheline appears unaltered and any analcimization is confined mainly to cleavages and crystal rims. Nepheline core compositions range from $Ne_{71}Ks_8Qz_{21}$ to more Si-rich $Ne_{62}Ks_4Qz_{34}$ (Table 2, No. 2; Fig. 1A). Rare wedge-shaped nephelines of presumed late crystallization are also Si-rich (Table 2, No. 1), as indeed are euhedral nepheline inclusions ($\sim 51\%\ SiO_2$) in interstitial analcime. However, early-crystallizing nephelines (inclusions in the rims of diopside phenocrysts) are also Si-rich,

Table 3 Analyses of analcimes *1* Average of 17 grains in analcime theralitc ST28 (Table 1, No.1), range in analcime SiO_2 = 48.27–50.64, *2* analcime in analcime theralite ST20, its formula calculated for 10(O) (natrolite formula) is $(CaKNa)_{1.95}(Fe^{3+}Al)_{2.03}Si_{2.98}O_{10}$, *3* average of 15 grains in analcime theralite ST20, range in analcime SiO_2 = 47.48–52.90, *4* relatively Si-rich analcime in analcime theralite ST20, *5* analcime in analcime tinguaite ST40, *6* analcime "inclusion" (after nepheline) in clinopyroxene phenocryst in analcime tinguaite ST12 (Table 1, No. 2), *7* average of 7 grains of groundmass analcime in analcime tinguaite ST12, *8* average of 6 grains of groundmass analcime in Portobello analcime tinguaite (Table 1, No. 3), *9* vug analcime coexisting with siderite and aegirine, Portobello analcime tinguaite, *10, 11* analcimes in Mount Nombi analcime-nepheline basanites (Table 1, Nos. 4 and 5, respectively), each analysis is the mean of 6 grains, *12* average of 9 grains of groundmass analcime, Spring Mount analcime mugearite (Table 1, No. 6)]

	Square Top								Portobello		Nombi		Spring Mount
Analysis number	1	Theralites 2	3	4	Tinguaites 5	6	7	8	9	10	11	12
SiO_2	49.48	47.48	50.66	56.10	49.97	50.34	53.74[a] (0.42)	54.71 (0.22)	60.20	53.72 (0.51)	55.04 (0.35)	53.06 (1.20)
Al_2O_3	26.39	26.96	25.63	22.21	25.24	24.70	23.40 (0.34)	22.90 (0.36)	18.61	22.96 (0.63)	22.80 (0.26)	24.27 (1.29)
Fe_2O_3	tr.	0.67	0.07	0.60	0.19	0.98	0.10 (0.09)	0.10 (0.07)	tr.	0.50 (0.25)	0.33 (0.11)	0.58 (0.25)
CaO	0.71	0.54	tr.	tr.	tr.	0.06	tr. –	tr. –	tr.	0.31 (0.26)	tr. –	0.77 (0.71)
Na_2O	14.83	15.55	15.08	12.96	15.95	15.27	14.27 (0.43)	14.18 (0.21)	11.54	13.46 (0.15)	12.92 (0.26)	12.50 (0.57)
K_2O	0.56	0.29	0.29	0.22	0.08	tr.	tr. –	tr. –	tr.	0.10 (0.01)	tr. –	0.97 (0.31)
Total	91.97	91.49	91.73	92.09	91.43	91.35	91.51	91.89	90.35	91.05	91.09	92.15
Cell formulae for 6(O)												
Si	1.843	1.789	1.881	2.042	1.871	1.884	1.981	2.005	2.196	1.988	2.022	1.950
Al	1.158 3.00	1.197 3.00	1.122 3.00	0.953 3.01	1.114 2.99	1.089 3.00	1.016 3.00	0.989 3.00	0.800 3.00	1.002 3.00	0.987 3.02	1.050 3.01
Fe^{3+}	–	0.018	0.001	0.016	0.005	0.027	0.003	0.003	–	0.014	0.009	0.014
Ca	0.028	0.022	–	–	–	0.002	–	–	–	0.012	–	0.030
Na	1.071	1.137	1.086	0.915	1.158	1.108	1.020	1.005	0.816	0.966	0.920	0.891
K	0.026	0.014	0.013	0.010	0.003	–	–	–	–	0.005	–	0.046
$Al + Fe^{3+}$	1.16	1.21	1.12	0.97	1.12	1.12	1.02	0.99	0.80	1.02	1.00	1.06
$2Ca + Na + K$	1.15	1.20	1.10	0.93	1.16	1.11	1.02	1.00	0.82	1.00	0.92	1.00
Mol%												
Ne	59.9	65.0	57.7	44.8	61.9	58.9	51.5	50.2	37.1	49.2	45.5	47.1
Ks	1.5	0.8	0.8	0.4	0.2	–	–	–	–	0.2	–	2.5
Qz	38.6	34.2	41.5	54.8	37.9	41.1	48.5	49.8	62.9	50.6	54.5	50.4

[a] ($\pm$ 1σ). Note: All analcimes are apparently devoid of 'relict' nepheline (compare Table 5)

$Ne_{58-62}Ks_{6-8}Qz_{36-30}$. Analcime is typically anhedral interstitial and may abut unaltered nepheline and alkali feldspar. Interstitial analcime is common in areas of late-crystallizing fine-grained mesostasis composed of alkali feldspar microlites, sodic pyroxene, nepheline and titanomagnetite. Biotite is a minor groundmass phase.

Tinguaites

The analcime tinguaites ST40 (DI = 71.3), ST16 (DI = 75.7) and ST12 (DI = 79.9) are clinopyroxene-alkali feldspar-nepheline-analcime-titanomagnetite assemblages (± olivine, arfvedsonite, natrolite). The major phenocryst phase is pinkish Mg-rich diopside (up to 4 mm; ST16, $Ca_{47}Mg_{40}\sum Fe_{13}$; ST_{12}, $Ca_{45}Mg_{38}\sum Fe_{17}$). Successive pyroxene generations are enriched in the aegirine component and the generalised pyroxene crystallization trend is from Mg-rich diopside phenocrysts (with sodian diopside rims) via aegirine augite to groundmass aegirine (with up to 13% Na_2O). Arfvedsonite is a minor groundmass phase (~ 1%) in tinguaites ST16 [mg = 54.6; mg = 100 Mg/(Mg + $\sum$ Fe)] and ST40 (mg = 34.3).

The alkali feldspars (4 mm in ST16, 0.5 mm in ST12) are sanidines (ST40, $Or_{50}Ab_{48}An_2$; ST16, $Or_{47}Ab_{53}$; ST12, $Or_{62}Ab_{38}$), often zoned to more Or-rich rims. For example, tinguaite ST16 feldspar core compositions range from $Or_{41}Ab_{59}$ to $Or_{48}Ab_{52}$ and rim compositions contain up to 10% more Or. The maximum compositional range within single crystals is found in tinguaite ST12 ($Or_{50}Ab_{50}$ to $Or_{87}Ab_{13}$).

Nepheline is both a phenocryst (1 mm) and groundmass phase. Sample ST16 alkali feldspar phenocrysts contain numerous nepheline euhedra. Some nepheline phenocrysts are zoned whereby, relative to core compositions, the rims are enriched in Si and Fe^{3+} and depleted in Al, Na, K (Table 2, Nos. 4C, 5R). Except for localized rim and cleavage alteration to analcime, phenocryst and groundmass nephelines generally appear fresh. There is no evidence of relict interstitial nepheline of late crystallization. Analcime is mainly a groundmass constituent, commonly as cloudy areas interstitial to alkali feldspars, or as pools of clear analcine. Natrolite is abundant in tinguaite ST16 where it replaces nepheline and sanidine.

Analcime tinguaite from the Dunedin Volcanic Complex, New Zealand

The tinguaite occurs as a dyke within the late Miocene Dunedin Volcanic Complex of East Otago, and is located on Portobello Peninsula in the middle reaches of Otago Harbour (Wilkinson 1968). It contains rare phenocrysts of nepheline (2 mm) and sodian hedenbergite $Ca_{46-47}Mg_{10-8}Fe_{44-45}$ in a fine-grained groundmass of prismatic Na-pyroxenes (aegirine augite and aegirine), alkali feldspar microlites, rare nepheline and abundant clear 'groundmass' analcime (~ 40–50%). Nephelines range in composition from relatively Si poor to Si rich types (Table 2, Nos. 6, 7) and phenocrysts may be zoned (Fig. 1C). Phenocryst and groundmass nephelines show only limited alteration to analcime. Groundmass analcime is stoichiometric $NaAlSi_2O_6$ of more-or-less constant composition (Table 3, No. 8). However, a more Si-rich analcime (60.2% SiO_2; Table 3, No. 9) occurs lining vugs (2 mm) where it is associated with aegirine and carbonates which include calcite (51% CaO), siderite (48% FeO) and ferroan rhodochrosite (41% MnO, 15% FeO). Alkali feldspar is sanidine, ranging in composition from $Ab_{60}Or_{40}$ to microlites as Or-rich as Ab_5Or_{95}.

Nombi basanites

The Nombi basanites (Table 1, Nos. 4, 5) are flows belonging to the Nombi Extrusives, an Upper Triassic-Lower Jurassic unit which crops out sporadically west of Gunnedah in north-eastern New South Wales (Bean 1974, 1975). The analysed samples have been termed basanites on the basis of their normative compositions ($AN > 50$, $ne > 5$) but they differ modally from typical basanites in which calcic plagioclase is a major phase. The low modal feldspar contents of the Nombi lavas (< 10 vol.%) are dominated by alkali feldspars. The SiO_2 and Al_2O_3 contents of these lavas are more typical of nephelinites.

Basanites R9687 (Table 1, No. 4) and R18720 (Table 1, No. 5) contain phenocrysts of zoned olivine (1.5 mm; Fo_{82-79}) variably altered to brownish green bowlingite, pink Mg-rich diopside (1 mm; $Ca_{50}Mg_{37-34}Fe_{13-16}$) in a groundmass of diopside ($Ca_{50}Mg_{34}Fe_{16}$), nepheline, analcime, alkali feldspars, Fe-Ti oxide, apatite, and minor biotite.

Unlike the nephelines and analcimes in the samples from the differentiated Square Top intrusion, the Nombi nephelines (Table 2, Nos. 8, 9; Fig. 1C) and analcimes (Table 3, Nos. 10, 11) have relatively constant compositions and nephelines are unzoned. Modal analcime exceeds nepheline in both samples (R18720 contains ~ 25 vol.% of analcime + nepheline). On purely textural grounds, the analcime appears primary because groundmass nephelines are often euhedral towards adjacent pools of analcime and analcimization of nepheline is limited.

Feldspar comprises only about 5% of basanite R9687 (which contains 0.08% BaO) and ranges in composition from barium potash oligoclase $Ab_{55}An_{24}Or_{15}Cn_6$ (3.0% BaO) to dominant anorthoclase as Or-rich as Or_{36} ($Ab_{54}Or_{36}An_6Cn_4$). Basanite R18720 (0.22% BaO) contains ~ 10% feldspars which include labradorite $Ab_{45}An_{51}Or_3Cn_1$ zoned to potash oligoclase $Ab_{62}An_{23}Or_{13}Cn_2$ and dominant alkali feldspars ranging from lime anorthoclase to barium sanidine $Ab_{42}Or_{50}An_4Cn_4$ (2.1% BaO).

Analcime mugearite from Spring Mount, north-eastern New South Wales

This early Oligocene flow contains high-pressure megacrysts of kaersutite, anorthoclase and Ti-rich biotite (Wilkinson and Hensel 1991). The mugearite carries phenocrysts (0.15 mm) of olivine Fo_{80} and potash oligoclase (2 mm) $Ab_{66}An_{27}Or_7$ in a very fine grained groundmass of Mg-rich diopside $Ca_{48}Mg_{34}Fe_{18}$, anorthoclase $Ab_{61}Or_{28}An_{11}$, sanidine $Ab_{28}Or_{70}An_2$, analcime, titanomagnetite and apatite. Analcime is the dominant groundmass phase, and its average composition is close to stoichiometric $NaAlSi_2O_6$ (Table 3, No. 12; Fig. 1C). Nepheline is absent.

Nepheline compositions and fractionation trends

With few exceptions, nepheline Qz components exceed those defining the limits of excess SiO_2 in solid solution in the system Ne-Ks-Qz-H_2O (nepheline-kalsilite-quartz-water) at 700° C and 1 kbar P_{H_2O} (Hamilton and MacKenzie 1960, Hamilton 1961), with the compositions of the most Qz-rich variants plotting in the stability field of nepheline plus feldspar (above the 1 bar 1068° C maximum; Figs 1, 2). Some nephelines in the Square Top theralites (e.g. Table 2, Nos. 1, 2) are among the most Si-rich on record. Compared with Ne and Qz, Ks displays only limited variation and An (anorthite) is a significant minor component only in the nephelines from the Nombi basanites (2.9–1.7 mol% An; Table 2, Nos. 8, 9) and in some nephelines from the most Ca-rich Square Top theralite (Table 1, No. 1), particularly those included in the rims of Ca-rich clinopyroxene (up to 2.2 An). The paucity of Ca can be

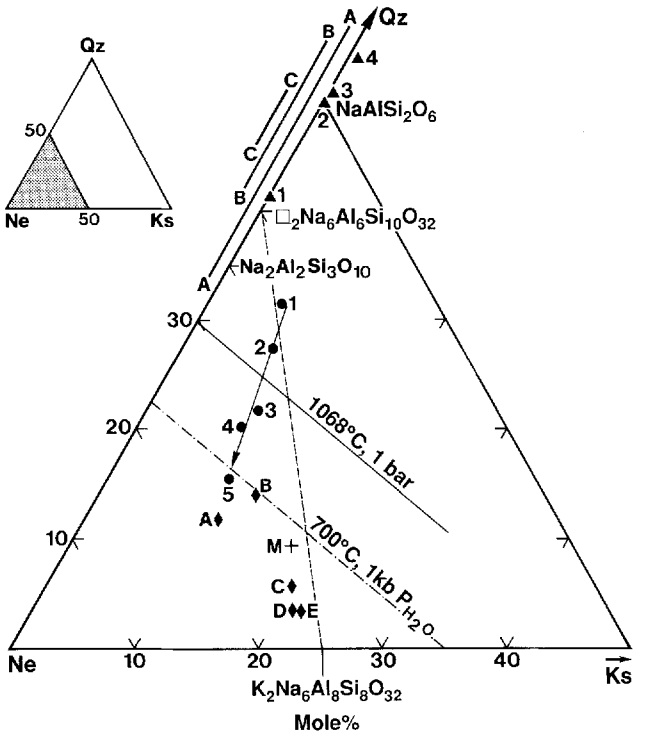

Fig. 2 Compositions of nephelines and analcimes, plotted as mole proportions of the components $NaAlSiO_4$ (Ne)-$KAlSiO_4$ (Ks)-SiO_2 (Qz), with the *dashed*, *solid* and *dot-dash* lines as in Fig. 1. The solid circles are "bulk" compositions of nephelines from the Square Top intrusion (Table 4). The trend *1* → *5* indicates the compositional trend of these nephelines with progressive fractionation. Analyses *5*, *A*, *B*, *C* denote the bulk compositions of nephelines from four salic alkaline heteromorphs (DI > 80) with different thermal histories. *5* Square Top tinguaite ST12 (nepheline-sanidine-analcime), rock co-ordinates in the Ne-Ks-Qz system $Ne_{50}Ks_{17}Qz_{33}$ wt%. A phonolite ($Ne_{48}Ks_{17}Qz_{35}$) from Dunedin, New Zealand (nepheline-anorthoclase; Tilley 1954). *B* average Norwegian lardalite ($Ne_{47}Ks_{20}Qz_{33}$). The orthoclase microperthite carries a monoclinic potassium phase (Tilley and Gittins 1961; Hamilton 1961). *C* nepheline syenite ($Ne_{46}Ks_{21}Qz_{33}$), Blue Mountain, Ontario (albite-microcline; Tiley 1952, 1954). *M* is the composition ($Ne_{73}Ks_{18}Qz_9$) which Morozewicz (1928) suggested to be the composition of natural nephelines. *D*, *E* are respectively the nepheline from a leucite nephelinite, Etinde, Cameroons West Africa and from a mariupolite, Vaal River, Transvaal (Tilley 1953). *Solid triangles* denote analcime compositions. *1* is the composition (~ $Ne_{59}Qz_{41}$) of analcime with the highest thermal stability (Peters et al. 1966; Liou 1971; Hamilton 1972; Roux and Hamilton 1976). *2* is the composition of $NaAlSi_2O_6$ analcime. Kim and Burley (1971) consider this to be the composition at the thermal trough of the analcime stability field. *3* is the average composition of 5 groundmass analcimes (this study, Table 3, Nos. 7, 8, 10, 11, 12). 4 is the average of 18 phenocryst analcimes ($Ne_{45}Ks_1Qz_{54}$), now widely interpreted as ion-exchanged leucites (Data sources: Crook 1967; Wilkinson 1968, 1977; Pearce 1970; Woolley and Symes 1976; Comin-Chiaramonti et al. 1979; Luhr and Kyser 1989; Karlsson and Clayton 1991). Note that the composition of analcime replacing leucite in a leucite tephrite from Roccamonfina, western Italy, is $Ne_{40}Ks_2Qz_{58}$ (Luhr and Kyser 1989). The *lines A-A*, *B-B*, *C-C* indicate the range of solid solution in analcimes derived from nepheline. A-A, this study; B-B, Barker and Hodges 1977; C-C Henderson and Gibb 1983

correlated with low Ca in the melt and/or the entry of Ca into other phases (diopside, plagioclase) crystallizing earlier or together with the nepheline.

Some Square Top and Portobello nephelines, mainly phenocrysts, are compositionally zoned, whereby Si (Qz) and Fe^{3+} increase and Al, Na (Ne), K (Ks) and Ca (An) decrease in the rims, relative to core compositions (Table 2). Henderson and Gibb (1983) have described similar zoning patterns in nephelines from small, high-level alkaline mafic intrusives. No cases of rims poorer in Si were observed in our samples. For Square Top nephelines, increases in Fe^{3+} in crystal rims and in successive nepheline fractions (Table 4) reflect increasing Fe^{3+}/Fe^{2+} melt ratios with fractionation and this trend is consistent with increases in the $NaFe^{3+}Si_2O_6$ component of successive pyroxene fractions.

If evolutionary trends for the Square Top and Portobello nephelines were to be based on zoning trends, the fractionation trends so deduced would be anomalous because they would imply that the rims crystallized at higher temperatures than the cores. They would in fact be the *opposite* to those defined by the "bulk" compositions of successive Square Top nepheline fractions which involve decreases in Qz and increases in Ne and Ks with increasing differentiation indices (and decreasing crystallization temperatures) of the respective hosts (Table 4 and Fig. 2).

It should be emphasized that the nepheline zoning depicted in Fig. 1 probably illustrates maximum compositional differences between cores and rims and that zoning, where detected, often just exceeds microprobe precision limits for Si, Al, etc. Furthermore, while we are unable to relate the compositions of individual nephelines unequivocally to a Square Top theralite crystallization sequence, we suspect that early- and late-crystallizing theralite nephelines probably do not differ significantly in composition. Thus early- crystallizing nepheline inclusions in diopside phenocrysts (average $Ne_{59}Ks_6Qz_{35}$) are similar in composition to (presumably late crystallizing) nephelines ($Ne_{62}Ks_5Qz_{33}$) interstitial to plagioclase laths. In Square Top tinguaites carrying nepheline phenocrysts it is clear from textural relations that nepheline crystallized before the major phase, namely alkali feldspar.

Zoning in nepheline involves an increase in the cavity cation vacancy and decreases in K and Na (K > Na), illustrated by the zoned nepheline in Table 2 (Nos. 4C, 5R). Following Donnay et al. (1959), the core and rim formulae (32O) of this nepheline are respectively $K_{1.10}Na_{6.35}\square_{0.55}(Al, Fe^{3+})_{7.51}Si_{8.50}O_{32}$ and $K_{0.82}Na_{6.21}\square_{0.97}(Al, Fe^{3+})_{7.02}Si_{8.98}O_{32}$ where $\square$ = cavity cation vacancy. In nepheline of ideal composition $K_2Na_6Al_8Si_8O_{32}$, the tridymite-type framework is distorted and the alkali sites are of two different sizes. As a result of the strong site preference in the nepheline structure, K-atoms are restricted to the two large cavities per unit cell while the six smaller cavities contain Na-atoms. "... the best evidence of the severity

Table 4 "Bulk" analyses of nephelines from theralites and tinguaites, Square Top intrusion. Nos. 1–4 are the means of *n* grains per specimen analysed by microprobe. No. 5 is a wet chemical analysis of nepheline separate from tinguaite ST12; total includes 0.72 H_2O (Wilkinson 1965). (*DI* differentiation index $\sum$ *or, ab, ne*)

Analysis number	Theralites 1	2	Tinguaites 3	4	5
Specimen number	ST28	ST20	ST40	ST16	ST12
SiO_2	50.62	49.62	47.86	47.41	45.27
Al_2O_3	30.08	30.30	30.89	30.91	31.81
Fe_2O_3	0.47	0.64	0.85	0.75	1.02
CaO	0.29	0.11	–	–	0.17
Na_2O	16.12	16.69	17.14	17.47	17.31
K_2O	2.42	2.81	3.35	3.05	3.48
Total	100.00	100.17	100.09	99.59	99.78
Cell formulae for 8 (O)					
Si	2.349	2.313	2.252	2.242	2.168
Al	1.645 4.01	1.664 4.00	1.713 4.00	1.723 3.99	1.795 4.00
Fe^{3+}	0.016	0.022	0.030	0.026	0.036
Ca	0.014	0.005	–	–	0.009
Na	1.450	1.508	1.563	1.602	1.607
K	0.143	0.167	0.201	0.183	0.212
[a]□	1.57	1.28	0.94	0.86	0.69
Mol%					
Ne	62.5	65.5	69.4	71.5	74.7
Ks	6.1	7.2	8.9	8.2	9.9
Qz	31.4	27.3	21.7	20.3	15.4
n	22	11	17	11	10
Range in nepheline SiO_2	51.82–48.95	51.95–46.16	49.70–46.16	48.66–46.21	47.66–44.71
Host rock DI	39.2	52.4	71.3	75.7	79.9

[a] Cavity cation vacancy □ (32 O) determined from the idealized nepheline formula $K_xNa_yCa_z\square_{8-(x+y+z)}Al_{x+y+2z}Si_{16-(x+y+2z)}O_{32}$ (Donnay et al. 1959)

of the structural problems produced by forcing Na to occupy the large cavity in nepheline is that, whenever possible, the problem is avoided through operation of a second cation replacement scheme involving substitution of Si for Al which then allows omission of an equal number of alkali atoms, found to be entirely from the large cavities" (Dollase and Thomas 1978). Hence a deficiency in nepheline rim K, relative to the core, should be coupled with an increase in rim Si at the expense of Al.

In projection, the salic components (less *an*) of the Square Top theralite-tinguaite sequence straddle the nepheline-feldspar field boundary in the Ne-Ks-Qz-H_2O system at 1 kbar P_{H_2O}. The tinguaites plot in the low-temperature trough located along this boundary (Wilkinson 1965, Fig. 4). Early crystallization of nepheline phenocryst cores would thus be followed by the crystallization of more abundant and increasingly more Or-rich alkali feldspars (the major phase in the tinguaites) and the crystallization histories of zoned Or-enriched feldspars and nepheline rims would overlap. Liquids would then be depleted in K (and Na) (for bulk alkali feldspars, K_2O ranges from 8.3 to 10.3 and Na_2O from 4.8 to 6.1). The nepheline rim compositions reflect this *localized* depletion in K and Na at advanced stages of nepheline crystallization.

The fractionation trend from theralite to tinguaite for *bulk* nephelines (Fig. 2) shows consistency with the microprobe "fields" (Fig. 1A, B) and involves a decrease in Qz and increases in Ne and Ks. This trend is largely temperature dependent because the amount of excess Si in solid solution in nepheline decreases with decreasing temperature (Fig. 2; Greig and Barth 1938; Hamilton 1961). Decreasing nepheline Si results in a decrease in □ (Table 4) and freer occupancy of the two larger cavities by K. Increasing Na and K in successive Square Top liquid fractions also enhanced the Na and K contents of successive bulk nepheline fractions.

Natural nepheline compositions and the Barth compositional join

Dollase and Thomas (1978) proposed a "compositional trend of naturally occurring nephelines" (= "natural nepheline compositional plane" of Barth, 1963), falling between the end-members $K_2Na_6Al_8Si_8O_{32}$ (the ideal composition of the unit cell; Hahn and Buerger 1955) and $\square_2Na_6Al_6Si_{10}O_{32}$. Dollase and Thomas (1978) related this trend (the Barth compositional join) to the strong site preferences in the nepheline structure. Henderson and Gibb (1983) noted that, although the most Qz-rich nephelines (with Qz greater than approximately 20) in their samples of high-level alkaline mafic intrusives plot close to the Barth join, nephelines with lower Qz contents (< Qz 20) are displaced to more

Ne-rich compositions. Henderson and Gibb (1983) commented that this compositional divergence might reflect the "syenitic" hosts of the nephelines considered by Dollase and Thomas (1978, Fig. 1) which "presumably coexist with potassic alkali feldspars" rather than the relatively sodic high-temperature feldspars in their alkaline mafic hosts.

The band of nepheline compositions defined by this study (Figs. 1, 2) broadly coincides with that documented by Henderson and Gibb (1983). This compositional field, extending from approximately $Ne_{62}Ks_4Qz_{34}$ to $Ne_{81}Ks_{15}Qz_4$ and encompassing the Square Top nepheline fractionation trend (Fig. 2), apparently defines the compositions of nephelines (more Na-rich than the ideal composition) which coexist with high-temperature alkali feldspars in a wide range of volcanic and subvolcanic mafic-felsic alkaline rocks. However, some felsic hosts such as the Square Top and Portobello tinguaites contain K-rich sanidines (as Or-rich as Or_{87-95}) and their nephelines still plot away from the Barth join towards Ne.

In view of the implication that the Barth join uniquely limits natural nepheline compositions (more Na-rich than the ideal composition) and the comment by Henderson and Gibb (1983), noted above, it is necessary to examine in more detail the various hosts of the nephelines defining the Dollase-Thomas trend. This is based on wet chemical and electron microprobe analyses which comply with nepheline-structure allowed stoichiometry (Bannister and Hey 1931).

The alkaline hosts are diverse in their mineralogies and thermal histories. Where adequate mineralogical data are available ($\sim$ 80% of the nephelines in question), the hosts can be assigned to three groups.

1. Extrusives and intrusives whose nephelines coexist with either: (a) a member of the high-temperature sanidine-anorthoclase (cryptoperthite) series; or (b) an intermediate thermal-state monoclinic potassium feldspar, including orthoclase microperthite. The extrusives are phonolites (Bowen and Ellestad 1936; Woolley and Symes 1976). Intrusives include a theralitic canadite (Tilley and Gittins 1961) but are mainly feldspatoidal syenites and tinguaites (Tilley 1954; Barth 1963; Wilkinson 1965; Heier 1966; Bose 1971; Henderson and Gibb 1972; Barker and Hodges 1977). With a few exceptions, their nephelines plot away from the Barth join towards Ne and occupy a somewhat diffuse field broadly comparable to those delineated by Henderson and Gibb (1983) and by this study. The exceptions include four nephelines reported by Bose (1971) and Barker and Hodges (1977), all of which fall on the Barth join ($Qz > 15$).

2. Slowly cooled hosts which include feldspathoidal syenites and nepheline "amphibolites" (Quinn 1937; Tilley 1952; Barker 1965; Sylvester and Anderson 1976), all of which carry low albite + microcline. Their nephelines plot on or adjacent to the Barth join.

3. Included in this group are extrusive and intrusive nepheline-clinopyroxene assemblages, devoid of plagioclase and alkali feldspar. Melilite nephelinites (Velde and Thiebaut 1973) and ijolites (Mitchell 1972; Rock 1976) are represented. Their nepheline compositions straddle the Barth join and differ from the nephelines in the previous groups by virtue of distinctly lower Qz components ($Qz < 5$).

Departures of Ne-rich nepheline compositions from the Barth join and variation in nepheline compositions on or close to this join can be attributed to several important controls on nepheline chemistry which include: the uniqueness of the Buerger ideal composition ($Ne_{75}Ks_{25}$ mol%, $Ne_{73}Ks_{27}$ wt.%), the physical conditions of nepheline crystallization, and the compositions of the various volcanic and subvolcanic hosts. Not only is the Buerger composition an end-member of the omission solid solution series $K_2Na_6Al_8Si_8O_{32}$-$\square_2Na_6Al_6Si_{10}O_{32}$ – it also marks the low-temperature termination of the sodium-rich limb of the nepheline-kalsilite solvus (Tuttle and Smith 1958). It also defines a limiting composition for low-temperature nephelines coexisting with low albite and microcline in slowly cooled plutonites and metamorphic assemblages. These typically range between $Ne_{75}Ks_{25}$ and $Ne_{73}Ks_{18}Qz_9$, the composition suggested by Morozewicz (1928) for natural nephelines (Fig. 2). This compositional range Tilley (1954) termed the Buerger-Morozewicz convergence field.

The uniqueness of the composition $K_2Na_6Al_8Si_8O_{32}$ at which all six sites suitable for Na atoms are filled is retained in the omission solid solution series along the Barth join which was defined originally for low-temperature natural nephelines (Barth 1963). However, for rapidly cooled volcanic and subvolcanic hosts containing high-temperature alkali feldspars, the tolerance of both alkali sites of the nepheline structure for greater departure from the ideal composition is increased.

The response by nepheline compositions to differing cooling histories is illustrated in Fig. 2 where the nephelines from four heteromorphic nepheline-alkali feldspar (-analcime) assemblages would change in composition by adjustment of K:Na ratios and by the replacement of Si by Al at lower crystallization temperatures (Tilley 1954). Thus assemblages with high-temperature alkali feldspars (Square Top tinguaite 5 and Dunedin phonolite A) would re-equilibrate to a low-temperature assemblage with albite-microcline (Blue Mountain nepheline syenite C) via intermediate temperatures (Norwegian lardalite B whose orthoclase microperthite carries a monoclinic potassic phase). The nephelines from some syenites with intermediate thermal-state feldspars (Bose 1971; Barker and Hodges 1977) plot on the Barth join at relatively high Qz (> 15). Lower temperature re-equilibration of these syenites to yield assemblages with low albite and microcline should yield a more Qz-poor nepheline in the convergence field.

The Qz-poor nephelines from feldspar-free melilite nephelinites and ijolites (group 3 above) may or may

not fall close to the Barth join and their compositions largely reflect those of their parent magmas. Quenched nephelines from melilite nephelinites lacking leucite may contain up to 37% Ks and Ks correlates positively with the K_2O/Na_2O ratios of the leucite-free hosts (Velde and Yoder 1978). Nephelines in the differentiates of melilite nephelinite can experience slight enrichment in Ks (Wilkinson and Stolz 1983).

Ijolitic nephelines also reflect host rock chemistries and the proximity of their compositions to the Ne-Ks join results from highly Si-deficient host compositions whose CIPW norms would contain *lc* ± *cs* (Nockolds 1954). Furthermore, ijolitic nephelines plotting in the convergence field are not necessarily indicative of low temperatures of crystallization, as sometimes suggested (e.g. Mitchell 1972). In this regard, the similar compositions of nephelines from chemically dissimilar hosts with quite different thermal histories, namely a feldspar-free leucite nephelinite (Fig. 2, sample D) and a microcline-bearing mariupolite (Fig. 2, sample E), may be noted.

When the physical and chemical controls of nepheline compositions are taken into account, the Barth compositional join is nevertheless important because it broadly delineates the compositional range of most natural nephelines which would be defined by the compositional band already noted, i.e. confined either to the join or to the Ne side of the join. Nephelines coexisting with feldspars in leucite-bearing hosts may also be more Ne-rich than the Buerger composition (Tilley 1958; Carmichael et al. 1974) and potassic nephelines ($> Ks_{25}$) appear to be largely restricted to the more K-rich highly Si deficient, feldspar-free melilite nephelinites (± leucite ± sodalite or haüyne ± kalsilite) (Bowen and Ellestad 1936; Velde and Yoder 1978). Nephelines in melilite nephelinites tend to be richer in Ks than those in relatively less silica-undersaturated nephelinites with similar K_2O/Na_2O ratios and hence the Ks contents of the respective nephelines may be functions of lava SiO_2 contents, as suggested by Velde and Yoder (1978). Nephelines plotting on the Ks side of the Barth join are apparently very rare in intrusives but they might be expected in the intrusive equivalent of melilite nephelinite (turjaite).

Analcime – composition and origin

The analcimes, especially those from the Square Top intrusion, display extensive solid solution along the Ne-Ab join (Figs. 1, 2) which largely reflects $NaAl \rightleftharpoons Si$ substitution. Their Si/Al ratios depart significantly from that of 'ideal' analcime $NaAlSi_2O_6$ (Si/Al = 2.0), with Si/Al ranging from 1.5 (Table 3, No. 2) to 2.7 (Table 3, No. 9). These ratios approach those defining the limits of solid solution in the analcimes synthesised by Saha (1959, 1961) in the system $NaAlSiO_4$-$NaAlSi_3O_8$-H_2O which range from ~ 1.4 to 3, i.e. from analcime of natrolite composition $NaAlSi_{1.5}O_5 \cdot 0.75H_2O$ to analcime of albite composition $NaAlSi_3O_8 \cdot 1.5H_2O$. On the other hand, the groundmass analcimes in the Portobello analcime tinguaite (Table 3, No. 8), the Nombi basanites (Nos. 10, 11) and Spring Mount mugearite (No. 12) display only limited grain-to-grain compositional variation and their average compositions are close to stoichiometric $NaAlSi_2O_6$ (Figs. 1C, 2). For all analcimes, K_2O is less than the maximum (~ 2% K_2O) indicated by experimental studies (Fudali 1963; Peters et al. 1966; Edgar 1978).

Studies of equilibrium phase relations in the system $NaAlSiO_4$-$KAlSiO_4$-SiO_2-H_2O and its sodic subsystems indicate that, for Na-rich silica-undersaturated compositions in the residua system, analcime and silicate melt cannot coexist above ~ 650° C or below about 5 kbar under water-saturated conditions (Peters et al. 1966; Morse 1968; Kim and Burley 1971; Roux and Hamilton 1976). The composition of analcime with the highest thermal stability at a given pressure is about $Ne_{50}Ab_{50}$ wt% (~ $Ne_{59}Qz_{41}$ mol%; Fig. 2) (Peters et al. 1966; Hamilton 1972; Roux and Hamilton 1976). The analcime composition at the thermal trough of its stability field seems to be stoichiometric $NaAlSi_2O_6$ (Kim and Burley 1971) and a majority of analcimes from igneous rocks approach this composition (Saha 1959, Fig. 4; Wilkinson 1968, Fig. 3; this paper, Fig. 2). The thermal stability of analcime of natrolite composition is apparently comparable with those of analcimes with slightly more Si-rich compositions (Saha 1961) and the stabilities of Ca-rich analcimes in some alkaline basic rocks are much reduced relative to that of Ca-free analcime in the Ne-Ab system (Henderson and Gibb 1977). There is some evidence that the thermal stability of relatively K rich analcimes might be increased relative to that of K-free variants (Peters et al. 1966) but this is not relevant to the K-poor analcimes in our samples.

The highly restrictive conditions of pressure, temperature and melt composition pose serious problems for a possible primary origin for any of the analcimes discussed here. The very fine grained nature of the Portobello and some Square Top tinguaites, the preservation of their high-temperature alkali feldspars, and the geological setting of the Portobello dyke within a supracrustal Miocene volcano preclude the crystallization of the Square Top and Portobello magmas at depths of more than 20 km (~ 5 kbar) below the contemporary surface. Emplacement of hydrous salic magmas at much shallower depths (P_{H_2O} = 1 kbar) does not resolve the P/T contains imposed by experimental data. Consider the "evolved" Square Top and Portobello tinguaites (Table 1, Nos. 2, 3) whose parameters in the residua system (wt%) are respectively $Ne_{50}Ks_{17}Qz_{33}$ and $Ne_{47}Ks_{18}Qz_{35}$, i.e. similar to those of the minimum melt composition in the Ab-Or-Ne-Ks-H_2O system at 1 kbar P_{H_2O} and 750° C ($Ne_{50}Ks_{19}Qz_{31}$; Hamilton and

MacKenzie 1965). At this water pressure, the solidus (760 ± 10° C) and liquidus 810 ± 10° C temperatures of a synthetic CaMgFe-free nepheline syenite composition $Ne_{46}Ks_{20}Qz_{34}$ (Barker 1965) still exceed those at which analcime is a potential primary phase from salic melts at much higher pressures. At 500 bars P_{H_2O} the solidus temperature of the synthetic nepheline syenite is 810 ± 10° C and at pressures up to 2 kbar P_{H_2O} its solidus temperatures also exceed those (~ 500–600° C) defining the reaction boundary: analcime ⇌ nepheline + albite + H_2O (Greenwood 1961; Liou 1971). It is unlikely that many *ne*-normative rock compositions would have a lower solidus temperature than that of the minimum melt composition in the residua system. Indeed, the solidus temperatures of the more mafic hosts (DI = 21–54) in Table 1 probably exceeded 1000° C (cf. Tilley et al. 1965; Thompson 1973). In this context it may be noted that analcime ($Ne_{54}Qz_{46}$) was eliminated from a Dippin Sill (Arran) crinanite above ~ 400° C (P_{H_2O} < 2 kbar; Henderson and Gibb 1977; Gibb and Henderson 1978).

Despite limited petrographic evidence of the nepheline-analcime conversion, we conclude that the interstitial and groundmass analcimes in our samples are subsolidus phases which formed from a precursor phase (nepheline) during interaction with deuteric and/or hydrothermal fluids. The question of precursor leucite does not arise – the hosts generally have distinctly sodic compositions and the low abundances of Rb (28–33 ppm) in the most potassic variant which is now devoid of nepheline (Table 1, No. 6) argue against the former presence of leucite in this lava. We also have no definitive evidence that clear, microscopically structureless groundmass analcime is a devitrification product of glass.

Silicon-rich nepheline is not necessarily a critical precursor to interstitial analcime (cf. Henderson and Gibb 1983) although such Si-rich nephelines should enhance the formation of Si-poor analcimes with the highest thermal stability (~ $Ne_{59}Qz_{41}$), i.e. those plotting near the composition of the theoretical K-free nepheline end-member of the Barth join (Figs. 1A, 2). Table 5 and Fig. 3 indicate that analcimes with compositions spanning a considerable range in solid solution may derive from relatively Si-poor nephelines, assuming that such analcime compositions have not been modified by later re-equilibration processes. Nevertheless, as pointed out by Henderson and Gibb (1983), the Si-rich nepheline-analcime reaction may be almost isochemical (Table 5, Nos. N1-A1; Fig. 1A). Note also that the compositions of Nombi analcimes reflect those of their parent nephelines whereby the more Qz-rich nepheline yields the more Qz-rich analcime (Fig. 1C).

Increasing SiO_2/Al_2O_3 molecular ratios of analcimes along the Ne-Qz join are consistent with decreasing crystallization temperatures (Liou 1971). The lowest temperature (deuteric) analcime analysed in this study is the unusually Si-rich variant (Table 3, No. 9) which coexists with carbonates and aegirine in a vug in the Portobello tinguaite. Cooper (1979) has described a Si-rich analcime (58.1% SiO_2; $Ne_{38}Ks_1Qz_{61}$) in an ocellus in a New Zealand lamprophyre. However, highly Si-rich analcimes such as the Portobello example typically occur in sedimentary and burial metamorphic rocks (Coombs and Whetten 1967).

It is interesting to note that the relatively Si-rich average composition of 18 analcime phenocrysts ($Ne_{45}Ks_1Qz_{54}$; Fig. 2) is one intrinsically more characteristic of relatively low crystallization temperatures. If these phenocrysts are intratelluric high-pressure phases which crystallized from melts at ~ 600° C (Roux and Hamilton 1976), then ideally their compositions should

Table 5 Analyses of nephelines and derivative analcimes. [Cations calculated on basis of 8 (O) for nephelines and 6 (O) for analcimes. *N* nepheline, *A* derivative analcime. *N1*, *A1* Nepheline phenocryst and its analcimized rim, analcime theralite ST28, Square Top intrusion (Table 1, No. 1), *N2*, *A2* relict nepheline in prismatic area of analcime, analcime tinguaite ST40, Square Top intrusion, *N3*, *A3* euhedral nepheline inclusion in alkali feldspar and its derivative analcime, analcime tinguaite ST40, Square Top intrusion, *N4*, *A4* rim of nepheline phenocryst and contiguous analcime, analcime tinguaite ST12, Square Top intrusion (Table 1, No. 2), *N5*, *A5*, *A5′* nepheline phenocryst N5 and analcime A5 between N5 and analcime A5′ at phenocryst rim, Portobello analcime tinguaite (Table 1, No. 3)]

Analysis number	N1	A1	N2	A2	N3	A3	N4	A4	N5	A5	A5′
SiO_2	50.37	50.26	47.83	46.85	47.92	51.17	47.87	53.48	45.79	50.07	55.10
Al_2O_3	29.89	25.11	31.84	26.76	31.57	24.80	31.40	23.37	32.11	26.64	22.02
Fe_2O_3	0.49	0.39	0.79	1.03	0.97	0.56	1.13	0.26	0.58	0.34	0.34
CaO	0.39	1.04	tr.	0.25	tr.	tr.	tr.	tr.	tr.	0.37	0.29
Na_2O	16.33	13.62	17.25	15.52	17.60	15.58	16.91	14.61	16.89	13.80	11.68
K_2O	2.46	0.70	3.73	1.02	3.67	0.34	3.45	tr.	4.42	1.78	1.80
Total	99.93	91.12	101.44	91.43	101.73	92.45	100.76	91.72	99.79	93.00	91.23
$Si + Al + Fe^{3+}$	4.00	3.00	4.00	3.00	3.99	2.99	4.01	3.00	4.00	3.02	3.01
$Al + Fe^{3+}$	1.66	1.12	1.77	1.23	1.76	1.10	1.77	1.02	1.82	1.17	0.97
2Ca + Na + K	1.66	1.11	1.78	1.21	1.80	1.11	1.74	1.04	1.83	1.09	0.95
Mol%											
Ne	64.0	54.9	70.0	65.0	71.3	59.0	70.9	53.0	71.6	54.3	41.6
Ks	6.3	1.9	9.9	2.8	9.8	0.8	9.5	–	12.3	4.6	4.2
Qz	29.7	43.2	20.1	32.2	18.9	40.2	19.6	47.0	16.1	41.1	54.2

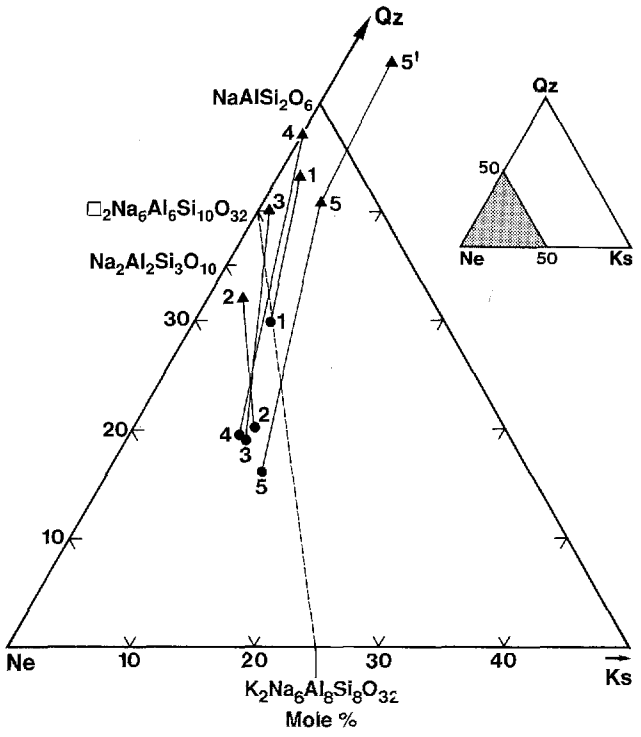

Fig. 3 Compositions of nephelines (*solid circles*) and derivative analcimes (*solid triangles*), plotted as mole proportions of the components $NaAlSiO_4$ (Ne)-$KAlSiO_4$ (Ks)-SiO_2 (Qz). *Tie lines 1-1, 2-2* etc. join "coexisting" phases whose compositions are listed in Table 5. The Dollase-Thomas (1978) nepheline trend is shown as a *dashed line*

approach the highest thermal stability composition ($Ne_{59}Qz_{41}$; ~ 51% SiO_2 for 8% H_2O). If these compositions (average analcime SiO_2 ~ 55% on a hydrous basis) are unmodified "pristine" compositions, they provide evidence of a low-temperature derivative origin as ion-exchanged leucites (leucite SiO_2 ~ 54%).

With the possible exception of the Spring Mount nepheline-free analcime mugearite whose high-pressure cognate kaersutite and Ti-rich mica megacrysts reflect the hydrous nature of the mugearite melt, the various magmas must have been strongly undersaturated in water, with the build up of magmatic water only becoming significant at near-solidus temperatures, when minor groundmass biotite (Square Top and Nombi) and arfvedsonite (Square Top) then crystallized as the only hydrous phases. The limited availability of magmatic water was largely responsible for the irregular distribution of analcime in some hosts and the survival of its precursor nepheline. Analcimization of nepheline probably occurred at temperatures below 450° C (Liou 1971). As already noted, the primary mineral assemblages of the Nombi "basanites" were olivine-clinopyroxene-nepheline, plus minor feldspar(s) and accessories. Analcimization of nepheline would have resulted in losses in whole rock Na_2O and K_2O and the norms of the original nephelinites would have contained more *or* and *ne* and less *ab* than the basanite norms in Table 1 (Nos. 4, 5).

Subsolidus analcimization therefore has the potential to convert nephelinites to analcimites. Similarly, high-level mafic intrusives such as crinanites and teschenites and their felsic associates such as analcime syenites may be interpreted as analcimized derivatives of nepheline-bearing dolerites and syenites. If analcime phenocrysts in alkaline volcanic and subvolcanic hosts are indeed ion-exchanged leucites and interstitial and groundmass analcimes are derivatives of nepheline, it would thus appear that few, if any, analcimes in alkaline igneous rocks are primary magmatic phases.

Acknowledgements We thank the Research School of Earth Sciences, Australian National University for access to the electron microprobe facility and N.G. Ware for analytical guidance. We also thank R.J. Arculus, D.S. Coombs, N.C.N. Stephenson and an anonymous reviewer for constructive comments on the manuscript.

References

Bannister FA, Hey MH (1931) A chemical, optical, and X-ray study of nepheline and kaliophilite. Mineral Mag 22:569–608

Barker DS (1965) Alkalic rocks at Litchfield, Maine. J Petrol 6:1–27

Barker DS, Hodges FN (1977) Mineralogy of intrusions in the Diablo Plateau, northern Trans-Pecos magmatic province, Texas and New Mexico. Geol Soc Am Bull 88:1428–1436

Barth TFW (1963) The composition of nepheline. Schweiz Mineral Petrog Mitt 43:153–164

Bean JM (1974) The geology and petrology of the Mullaley area of New South Wales. J Geol Soc Aust 21:63–72

Bean JM (1975) Petrology and petrochemistry of igneous rocks in the Mullaley area of New South Wales. J Proc R Soc NSW 108:131–146

Bose MK (1971) Petrology of the nepheline syenite of Mount Girnar, India. Lithos 4:357–366

Bowen NL, Ellestad RB (1936) Nepheline contrasts. Am Mineral 21:363–368

Carmichael ISE, Turner FJ, Verhoogen J (1974) Igneous petrology. McGraw-Hill, New York, USA

Coleman AP (1899) A new analcite rock from Lake Superior. J Geol 7:431–436

Comin-Chiaramonti P, Meriani S, Mosca R, Sinigoi S (1979) On the occurrence of analcime in the northeastern Azerbaijan volcanics (northwestern Iran). Lithos 12:187–198

Coombs DS, Whetten JT (1967) Composition of analcime from sedimentary and burial metamorphic rocks. Geol Soc Am Bull 78:269–282

Cooper AF (1979) Petrology of ocellar lamprophyres from west Otago, New Zealand. J Petrol 20:139–163

Crook KAW (1967) Analyses of five analcimes from North America. Geol Soc Am Bull 78:280–282

Dollase WA, Thomas WM (1978) The crystal chemistry of silica-rich, alkali-deficient nepheline. Contrib Mineral Petrol 66:311–318

Donnay G, Schairer JF, Donnay JDH (1959) Nepheline solid solutions. Mineral Mag 32:93–109

Edgar AD (1978) Subsolidus phase relations in the system $NaAlSi_2O_6$-$KAlSi_2O_6$ at 1 kbar P_{H_2O} and their bearing on the origin of pseudoleucites and analcime in igneous rocks. Neues Jahrb Mineral Monatsh 5:210–222

Edgar AD (1979) Shackanite and related analcite-bearing lavas in British Columbia:Discussion. Can J Earth Sci 16:1298–1299

Ferguson LJ, Edgar AD (1978) The petrogenesis and origin of the analcime in the volcanic rocks of the Crowsnest Formation, Alberta. Can J Earth Sci 15:69–77

Fudali RF (1963) Experimental studies bearing on the origin of pseudoleucite and associated problems of alkalic rock systems. Geol Soc Am Bull 74:1101–1125

Gibb FGF, Henderson CMB (1978) The petrology of the Dippin sill, Isle of Arran. Scott J Geol 14:1–27

Greenwood HJ (1961) The system $NaAlSi_2O_6$-H_2O-argon:total pressure and water pressure in metamorphism. J Geophys Res 66:3923–3946

Greig JW, Barth TFW (1938) The system $Na_2O \cdot Al_2O \cdot 2SiO_2$ (nephelite, carnegieite) – $Na_2O \cdot Al_2O_3 \cdot 6SiO_2$ (albite). Am J Sci 35A:93–112

Gupta AK, Fyfe WS (1975) Leucite survival:the alteration to analcime. Can Mineral 13:361–363

Hahn T, Buerger MJ, (1955) The detailed structure of nepheline, $KNa_3Al_4Si_4O_{16}$. Z Kristallogr 106:308–338

Hamilton DL (1961) Nephelines as crystallization temperature indicators. J Geol 69:321–329

Hamilton DL (1972) The system $NaAlSi_3O_8$(Ab)-$NaAlSiO_4$(Ne)-H_2O at 8 and 12 kilobars. NERC Prog Exp Petrol 2:24–27

Hamilton DL, MacKenzie WS (1960) Nepheline solid solution in the system $NaAlSiO_4$-$KAlSiO_4$-SiO_2. J Petrol 1:56–72

Hamilton DL, MacKenzie WS (1965) Phase equilibrium studies in the system $NaAlSiO_{4i}$ (nepheline)-$KAlSiO_4$ (kalsilite)-SiO_2-H_2O. Mineral Mag 34:214–231

Heier KS (1966) Some crystallochemical relations of nephelines and feldspars on Stjernöy, North Norway. J Petrol 7:95–113

Henderson CMB, Gibb FGF (1972) Plagioclase – Ca-rich-nepheline intergrowths in a syenite from the Marangudzi complex, Rhodesia. Mineral Mag 38:670–677

Henderson CMB, Gibb FGF (1977) Formation of analcime in the Dippin sill, Isle of Arran. Mineral Mag 41:534–537

Henderson CMB, Gib FGF (1983) Felsic mineral crystallization trends in differentiating alkaline basic magmas. Contrib Mineral Petrol 84:355–364

Karlsson HR, Clayton RN (1991) Analcime phenocrysts in igneous rocks: primary or secondary? Am Mineral 76:189–199

Kim KT, Burley BJ (1971) Phase equilibria in the system $NaAlSi_3O_8$-$NaAlSiO_4$-H_2O with special emphasis on the stability of analcite. Can J Earth Sci 8:311–337

Liou JG (1971) Analcime equilibria. Lithos 4:389–402

Luhr JF, Kyser TK (1989) Primary igneous analcime: the Colima minettes. Am Mineral 74:216–223

Mitchell RH (1972) Composition of nepheline, pyroxene and biotite in ijolite from the Seabrook Lake complex, Ontario, Canada. Neues Jharb Mineral Monatsh 9:415–422

Morimoto N (1988) Nomenclature of pyroxenes. Am Mineral 73:1123–1133

Morozewicz J (1928) Über die chemische Zusammensetzung des gesteinbildenden nephelins. Fennia 22:1–16

Morse SA (1968) Syenites. Carnegie Inst Washington Yearb 67:112–120

Nakamura Y, Yoder HS (1974) Analcite, hyalophane, and phillipsite from the Highwood Mountains, Montana. Carnegie Inst Washington Yearb 73:354–358

Nockolds SR (1954) Average chemical compositions of some igneous rocks. Geol Soc Am Bull 65:1007–1032

Pearce TH (1970) The analcite-bearing volcanic rocks of the Crowsnest Formation, Alberta. Can J Earth Sci 7:46–66

Pearce TH (1993) Analcime phenocrysts in igneous rocks: primary or secondary? – Discussion. Am Mineral 78:225–229

Peters Tj, Luth WC, Tuttle OF (1966) The melting of analcite solid solutions in the system $NaAlSiO_4$-$NaAlSi_3O_8$-H_2O. Am Mineral 51:736–753

Pirsson LV (1986) On the monchiquites or analcite group of igneous rocks. J Geol 4:679–690

Quinn A (1937) Petrology of the alkaline rocks at Red Hill, New Hampshire. Geol Soc Am Bull 48:373–402

Rock NMS (1976) Petrogenetic significance of some new xenolithic alkaline rocks from East Africa. Mineral Mag 40:611–625

Rock NMS (1977) The nature and origin of lamprophyres: some defintions, distinctions, and derivations. Earth-Sci Rev 13:123–169

Roux J, Hamilton DL (1976) Primary igneous analcite – an experimental study. J Petrol 17:244–257

Saha P (1959) Geochemical and X-ray investigation of natural and synthetic analcites. Am Mineral 44:300–313

Saha P (1961) The system $NaAlSiO_4$ (nepheline)-$NaAlSi_3O_8$ (albite)-H_2O. Am Mineral 46:859–884

Sylvester GC, Anderson GM (1976) The Davis nepheline syenite and associated nepheline gneisses near Bancroft, Ontario. Can J Earth Sci 13:249–265

Thompson RN (1973) One-atmosphere melting behaviour and nomenclature of terrestrial lavas. Contrib Mineral Petrol 41:197–204

Tilley CE (1952) Nepheline parageneses. Sir Douglas Mawson Anniversary Vol., Univ Adelaide, 167–177

Tilley CE (1953) The nephelinite of Etinde, Cameroons West Africa. Geol Mag 90:145–151

Tilley CE (1954) Nepheline-alkali feldspar parageneses. Am J Sci 252:65–75

Tilley CE (1958) The leucite nepheline dolerite of Meiches, Vogelsberg, Hessen. Am Mineral 43:758–761

Tilley CE, Gittins J (1961) Igneous nepheline-bearing rocks of the Haliburton-Bancroft province of Ontario. J Petrol 2:38–48

Tilley CE, Yoder HS, Schairer JF (1965) Melting relations of volcanic tholeiite and alkali rock series. Carnegie Inst Washington Yearb 64:69–82

Tuttle OF, Smith JV (1958) The nepheline-kalsilite system. II. Phase relations. Am J Sci 256:571–589

Velde D, Thiebaut J (1973) Quelques précisions sur la constitution minéralogique de la néphélinite à olivine et mélilite d'Essey-la-Côte (Meurthe-et-Moselle). Bull Soc Fr Mineral Cristallogr 96:298–302

Velde D, Yoder HS (1978) Nepheline solid solutions in melilite-bearing eruptive rocks and olivine nephelinites. Carnegie Inst Washington Yearb 77:761–767

Ware NG (1991) Combined energy-dispersive and wavelength-dispersive quantitative electron microprobe analysis. X-Ray Spectrom 20:73–79

Washington HS (1898) Sölvsbergite and tinguaite from Essex Country, Mass, Am J Sci 156:176–187

Wilkinson JFG (1965) Some feldspars, nephelines and analcimes from the Square Top intrusion, Nundle, N.S.W. J Petrol 6:420–444

Wilkinson JFG (1966) Clinopyroxenes from the Square Top intrusion, Nundle, New South Wales. Mineral Mag 35:1061–1070

Wilkinson JFG (1968) Analcimes from some potassic igneous rocks and aspects of analcime-rich igneous asemblages. Contrib Mineral Petrol 18:252–269

Wilkinson JFG (1977) Analcime phenocrysts in a vitrophyric analcimite – primary or secondary? Contrib Mineral Petrol 64:1–10

Wilkinson JFG, Hensel HD (1991) An analcime mugearite-megacryst association from north-eastern New South Wales: implications for high-pressure amphibole-dominated fractionation of alkaline magmas. Contrib Mineral Petrol 109:240–251

Wilkinson JFG, Stolz AJ (1983) Low-pressure fractionation of strongly undersaturated alkaline ultrabasic magma: the olivine-melilite nephelinite at Moiiili, Oahu, Hawaii. Contrib Mineral Petrol 83:363–374

Wooley AR, Symes RF (1976) The analcime-phyric phonolites (blairmorites) and associated analcime kenytes of the Lupata Gorge, Mocambique. Lithos 9:9–15